

# Time-dependent Gutzwiller theory of pairing fluctuations in the Hubbard model

G. Seibold,<sup>1</sup> F. Becca,<sup>2</sup> and J. Lorenzana<sup>3</sup>

<sup>1</sup>*Institut für Physik, BTU Cottbus, PBox 101344, 03013 Cottbus, Germany*

<sup>2</sup>*CNR-INFM Democritos, National Simulation Centre, and SISSA I-34014 Trieste, Italy.*

<sup>3</sup>*Center for Statistical Mechanics and Complexity, INFM, Dipartimento di Fisica, Università di Roma La Sapienza, P. Aldo Moro 2, 00185 Roma, Italy*

(Dated: November 29, 2018)

We present a method to compute pairing fluctuations on top of the Gutzwiller approximation (GA). Our investigations are based on a charge-rotational invariant GA energy functional which is expanded up to second order in the pair fluctuations. Equations of motion for the fluctuations lead to a renormalized ladder type approximation. Both spectral functions and corrections to static quantities, like the ground-state energy, are computed. The quality of the method is examined for the single-band Hubbard model where we compare the dynamical pairing correlations for s- and d-wave symmetries with exact diagonalizations and find a significant improvement with respect to analogous calculations done within the standard Hartree-Fock ladder approximation. The technique has potential applications in the theory of Auger spectroscopy, superconductivity, and cold atom physics.

PACS numbers: 71.10.Fd, 71.30.+h, 79.20.Fv

## I. INTRODUCTION

The present interest in the physics of strongly correlated fermion systems is accompanied by a ‘revival’ of the Gutzwiller wave function (GWF)<sup>1</sup> in order to study Hubbard-type models. In these Hamiltonians, doubly occupied sites contribute with an energy  $U$  to the total energy, though their weight is partially reduced by the Gutzwiller projector. Originally, the projector was applied to a Slater determinant describing a spatially uniform Fermi liquid. Along the years, states with long-range order have been considered, including projected BCS wave functions,<sup>2,3,4,5</sup> used in the context of high- $T_c$ .

Analytic evaluations of expectation values using the GWF are only possible in one<sup>6</sup> and infinite dimensions.<sup>7,8</sup> In the latter limit, one recovers the so-called Gutzwiller approximation (GA) first introduced by Gutzwiller himself in Ref. 9. The GA, later on rederived as a saddle-point within a slave-boson formulation of the Hubbard model,<sup>10</sup> yields an energy functional for quasiparticles with renormalized hopping amplitude. Therefore, it offers a simple and intuitive picture for the interplay between local correlation and electron kinetics and it is used in a variety of fields including the description of inhomogeneous states in cuprates,<sup>11</sup> band structure calculations,<sup>12</sup> and the theory of He<sup>3</sup>.<sup>13</sup>

In the past few years, two of us have developed a scheme which allows the computation of Gaussian fluctuations on top of the GA.<sup>14,15,16</sup> Within this so-called time-dependent GA (TDGA), it is possible to evaluate dynamical correlation functions in the charge and spin channel, which over a wide parameter regime are in good agreement with exact diagonalization results and constitute a significant improvement over the traditional Hartree-Fock plus Random-phase approximation (HF+RPA). The TDGA has been used in order to compute dynamical properties of inhomogeneous states in

cuprates. Results obtained in this way for the optical conductivity<sup>17</sup> and magnetic susceptibility<sup>18,19</sup> of stripe ordered phases have turned out to be in excellent agreement with experimental data.

In the present paper, we generalize the TDGA towards the inclusion of pairing fluctuations. The significance of such correlations is probably most prominent in the context of superconductivity where the appearance of a singularity in the pair susceptibility signals the onset of Cooper-pair condensation. Here, we aim to study the spectrum of pairing correlations in the normal state of the Hubbard model, an issue which has also been addressed, among others, within exact diagonalization<sup>20,21</sup> and various Monte Carlo methods.<sup>22,23,24,25,26,27,28</sup> In the particle-hole channel, the coupling to an electric or magnetic field yields the optical conductivity and magnetic susceptibility, respectively. In the particle-particle channel, direct measurements of pairing correlations are not so common since they do not couple to a classical field. However, principles for the measurement of the pair susceptibility in metals have been discussed in Refs. 29,30,31,32. The basic idea is to probe the fluctuating pair field of a metal in the normal state which is coupled to a superconductor via the tunnel current-voltage characteristics. In addition, the pairing correlation function for local pairs is the main ingredient in the theory of Auger spectroscopy<sup>33,34,35,36</sup> and also has relevance in the field of ultra-cold atom physics.<sup>37</sup>

In materials which can be described within Hubbard-type models, a strong local repulsion induces so-called antibound states (also known as two-particle resonances), above the two-particle continuum. The resonances appear as atomic-like features in the Auger spectrum. In Ref. 38 we have shown that, despite its computational simplicity, the TDGA yields an excellent description of the two-particle response. In particular, it describes well the energy gap between band and antibound states and

the relative spectral weight even far from the dilute limit in contrast to the ‘bare ladder approximation’ (BLA), which is restricted to the low-density regime.<sup>39,40</sup> Thus, the TDGA allows one to extend ladder-type theories much beyond their supposed limit of validity. The result is an effective ladder theory where quasiparticles get heavier, as usual due to correlations, and at the same time the effective interactions between quasiparticles become strongly renormalized. These vertex and self-energy corrections are consistent with each other and do not suffer from the pitfalls frequently found in diagrammatic computations, where an improvement at the level of the self-energy alone leads to a degradation of the overall performance of the theory due to the lack of appropriate vertex corrections.<sup>35,36</sup>

In this paper, besides a thorough derivation of the ‘pairing TDGA’, we extend the approach to intersite correlations with extended s-wave and d-wave symmetry. We will show that the TDGA yields an effective interaction between quasiparticles which is renormalized with respect to the bare  $U$  due to correlations but it does not include enough fluctuation effects to induce a superconducting instability. This is because we start from a paramagnetic state treated in the GA which does not have enough variational freedom to describe the scale  $J$  of magnetic fluctuations. In addition, within the RPA treatment for a paramagnet the particle-particle and particle-hole channel are decoupled and do not influence each other. For spin-density wave ground states, the TDGA induces attractive interactions between nearest-neighbor pairs which are not present in the HF approach based on BLA. However, these are not enough to produce a superconducting instability. Superconductivity due to an electronic mechanism requires the feedback of particle-hole fluctuations on the particle-particle channel and this goes beyond our approach. On the other hand, at the level of spectroscopic quantities this is a minor effect and our approach turns out to be in excellent agreement with exact diagonalizations. Here and below we use the terms “ladder-type fluctuations”, “particle-particle RPA fluctuations” and “pairing fluctuations” as synonymous.

This paper is organized as follows: The formalism is presented in detail in Sec. II where as a first step we derive the charge-rotational invariant GA functional from the Hubbard model in Sec. II A. Based on this functional, we show in Sec. II B how ladder-type fluctuations can be incorporated into the approach and how dynamical pair correlations can be computed. Results are presented in Sec. III where we first exemplify the method by means of a two-site model. Then the dynamical pairing correlations for different symmetries are computed on small clusters and compared with exact diagonalization results and HF+BLA computations. Finally, we conclude our investigations in Sec. IV.

## II. FORMALISM

### A. Charge-rotationally invariant GA

The starting point is the one-band Hubbard model:

$$H = \sum_{i,j,\sigma} (t_{ij} - \mu\delta_{ij}) c_{i\sigma}^\dagger c_{j\sigma} + U \sum_i \hat{n}_{i\uparrow} \hat{n}_{i\downarrow}, \quad (1)$$

where  $c_{i\sigma}$  ( $c_{i\sigma}^\dagger$ ) destroys (creates) an electron with spin  $\sigma$  at site  $i$ , and  $\hat{n}_{i\sigma} = c_{i\sigma}^\dagger c_{i\sigma}$ .  $U$  is the on-site Hubbard repulsion,  $t_{ij}$  denotes the hopping parameter between sites  $i$  and  $j$  and  $\mu$  is the chemical potential.

The Gutzwiller variational wave function can be written as

$$|\Phi_G\rangle \equiv \prod_i \hat{P}_i |\phi\rangle, \quad (2)$$

where  $\hat{P}_i$  partially projects out a doubly occupied state at site  $i$  from the uncorrelated wave function  $|\phi\rangle$ . In the traditional Gutzwiller approach,<sup>1</sup> the latter is a Slater determinant and the associated density matrix only contains the normal part:

$$\rho_{ij}^{\sigma\sigma'} \equiv \langle \phi | c_{j\sigma'}^\dagger c_{i\sigma} | \phi \rangle.$$

Here, we will consider a more general formulation in which  $|\phi\rangle$  is a Bogoliubov vacuum and define the anomalous part of the density matrix

$$\kappa_{ij} \equiv \langle \phi | c_{j\downarrow} c_{i\uparrow} | \phi \rangle.$$

In the general case the normal part can describe charge-density wave and spin-density wave broken symmetries. We will allow the ground state to have these broken symmetries but we will assume it is normal so our saddle point anomalous density matrix will vanish. We denote quantities at the saddle point by a 0, thus  $\kappa_{ij}^0 = 0$ . The anomalous part is important in order to obtain the fluctuations. Indeed, in the following, we consider an external time-dependent perturbation which induces pairing fluctuations on  $|\phi\rangle$ , then the instantaneous  $|\phi\rangle$  will take a BCS-like form.

The charge-rotationally invariant Gutzwiller functional for general charge and spin textures is derived in the Appendix A exploiting the well known equivalence between the slave-boson method and the Gutzwiller approach and following previous works.<sup>41,42,43,44,45</sup> Alternatively, one can use a pure Gutzwiller formulation with an appropriate projector  $\hat{P}_i$ .<sup>46</sup> The generalized energy functional for the Hubbard model reads:

$$F(\rho, \kappa, D) = \sum_{i,j} t_{ij} \langle \phi | \Psi_i^\dagger \mathbf{A}_i \boldsymbol{\tau}_z \mathbf{A}_j \Psi_j | \phi \rangle - \mu \sum_i \rho_{ii} + U \sum_i D_i, \quad (3)$$

which depends on the normal and anomalous parts of the density matrix and the variational double occupancy

parameters  $D_i$ . In Eq. (3),  $\rho_{ii} \equiv \sum_{\sigma} \rho_{ii}^{\sigma\sigma}$  and we have introduced Nambu notation

$$\Psi_i^\dagger = (c_{i\uparrow}^\dagger, c_{i\downarrow}) \quad \Psi_i = \begin{pmatrix} c_{i\uparrow} \\ c_{i\downarrow}^\dagger \end{pmatrix}. \quad (4)$$

It is also convenient to define the following pseudospin vector

$$J_i^x = \frac{1}{2} \Psi_i^\dagger \tau_x \Psi_i = \frac{1}{2} (c_{i\uparrow}^\dagger c_{i\downarrow}^\dagger + c_{i\downarrow} c_{i\uparrow}), \quad (5)$$

$$J_i^y = \frac{1}{2} \Psi_i^\dagger \tau_y \Psi_i = -\frac{i}{2} (c_{i\uparrow}^\dagger c_{i\downarrow}^\dagger - c_{i\downarrow} c_{i\uparrow}), \quad (6)$$

$$J_i^z = \frac{1}{2} \Psi_i^\dagger \tau_z \Psi_i = \frac{1}{2} (c_{i\uparrow}^\dagger c_{i\uparrow} + c_{i\downarrow}^\dagger c_{i\downarrow} - 1), \quad (7)$$

where  $\tau_i$  denote the Pauli matrices. The components of  $\vec{J}_i$  obey the standard commutation relations of a spin

1/2 algebra. We use boldface letter to indicate two-component vectors and  $2 \times 2$  matrices in Nambu space, whereas we denote Cartesian vectors by using an arrow.

The raising and lowering operators are defined as

$$J_i^+ = J_i^x + iJ_i^y = c_{i\uparrow}^\dagger c_{i\downarrow}^\dagger, \quad (8)$$

$$J_i^- = J_i^x - iJ_i^y = c_{i\downarrow} c_{i\uparrow}. \quad (9)$$

Within these definitions the matrix  $\mathbf{A}_i$  in Eq. (3) reads as

$$\mathbf{A}_i = \begin{pmatrix} \frac{z_{i\uparrow} + z_{i\downarrow}}{2} + \frac{z_{i\uparrow} - z_{i\downarrow}}{2} \frac{\langle J_i^z \rangle}{\langle J_i \rangle} & \frac{\langle J_i^- \rangle}{2\langle J_i \rangle} [z_{i\uparrow} - z_{i\downarrow}] \\ \frac{\langle J_i^+ \rangle}{2\langle J_i \rangle} [z_{i\uparrow} - z_{i\downarrow}] & \frac{z_{i\uparrow} + z_{i\downarrow}}{2} - \frac{z_{i\uparrow} - z_{i\downarrow}}{2} \frac{\langle J_i^z \rangle}{\langle J_i \rangle} \end{pmatrix}, \quad (10)$$

and all expectation values  $\langle \dots \rangle$  refer to the state  $|\phi\rangle$ . The Gutzwiller renormalization factors are given by

$$z_{i\sigma} = \frac{\sqrt{D_i - \langle J_i^z \rangle - \langle J_i \rangle} \sqrt{1/2 + \langle J_i^z \rangle - D_i + \sigma \langle S_i^z \rangle} + \sqrt{1/2 + \langle J_i^z \rangle - D_i - \sigma \langle S_i^z \rangle} \sqrt{D_i - \langle J_i^z \rangle + \langle J_i \rangle}}{\sqrt{1/4 - (\langle J_i \rangle + \langle S_i^z \rangle)^2}}. \quad (11)$$

Note that in the limit  $\langle J_i^\pm \rangle = 0$ , where the matrix  $\mathbf{A}_i$  is diagonal, one recovers the standard Gutzwiller energy functional as derived by Gebhard<sup>8</sup> or Kotliar-Ruckenstein:<sup>10</sup>

$$F(\rho, D) = \sum_{i,j} t_{ij\sigma} z_{i\sigma} z_{j\sigma} \rho_{ji}^{\sigma\sigma} - \mu \sum_i \rho_{ii} + U \sum_i D_i, \quad (12)$$

with the hopping renormalization factors

$$z_{i\sigma} = \frac{\sqrt{(\rho_{ii}^{\sigma\sigma} - D_i)(1 - \rho_{ii} + D_i)} + \sqrt{(\rho_{ii}^{\bar{\sigma}\bar{\sigma}} - D_i)D_i}}{\sqrt{\rho_{ii}^{\sigma\sigma}(1 - \rho_{ii}^{\sigma\sigma})}}. \quad (13)$$

The minimization of the energy functional of Eq. (3) leads to the stationary Gutzwiller wave function and to the associated stationary uncorrelated state  $|\phi_0\rangle$ .

## B. Calculation of pair fluctuations around general GA saddle points

The energy functional of Eq. (3) is a convenient starting point for the calculation of pair excitations on top of unrestricted Gutzwiller wave functions. Following the general approach of Refs. 14,15,16,38, we study the response of the system to an external time-dependent perturbation which induces small-amplitude oscillations in the particle-particle channel:

$$\mathcal{F}(t) = \sum_i (f_{ij} e^{-i\omega t} c_{i\downarrow} c_{j\uparrow} + H.c.). \quad (14)$$

Correspondingly, we have to expand the energy functional of Eq. (3) around the stationary solution up to

second order in the density and double-occupancy deviations. As already mentioned, we shall restrict to saddle-point solutions in the normal state:

$$\kappa_{ij}^0 = \langle J_i^+ \rangle_0 = \langle J_i^- \rangle_0 = 0, \quad (15)$$

and we remind the reader that a subscript or superscript 0 indicates quantities evaluated in the stationary state  $|\phi_0\rangle$ . Fluctuations are defined as  $\delta\rho(t) = \rho(t) - \rho_0$ , etc.

In the present case, particle-hole (ph) and particle-particle (pp) sectors in the expansion are decoupled and one obtains

$$F = F_0 + \text{tr}\{h^0 \delta\rho\} + \delta F^{\text{ph}} + \delta F^{\text{pp}}, \quad (16)$$

where we have introduced the Gutzwiller Hamiltonian:<sup>47,48</sup>

$$h_{ij}^{\sigma\sigma'}[\rho, D] = \frac{\partial F}{\partial \rho_{ji}^{\sigma'\sigma}} \delta_{\sigma,\sigma'}. \quad (17)$$

This coincides with the Kotliar-Ruckenstein Hamiltonian matrix.<sup>10</sup> In particular, the diagonal elements (in the basis of atomic orbitals) coincide with the Lagrange multipliers of the Kotliar-Ruckenstein method,  $\Sigma_{i\sigma}$ , after adding the chemical potential:

$$\Sigma_{i\sigma} = \frac{\partial F}{\partial \rho_{ii}^{\sigma\sigma}} + \mu. \quad (18)$$

In Ref. 38 we have interpreted  $\Sigma_{i\sigma}$  as a local GA self-energy.

Since we have included  $\mu$  in Eq. (1) the eigenvalues of Eq. (17),  $\xi$ , describe the single-particle excitations with

respect to the chemical potential at the GA level. We denote the particle (hole) energies above (below) the Fermi energy by  $\xi_{p\sigma}$  ( $\xi_{h\sigma}$ ) with  $\xi_{p\sigma} > 0 > \xi_{h\sigma}$ .

The transformation from real space fermions  $c_{i\sigma}$  to GA operators is written as

$$c_{i\sigma} = \sum_p \phi_{i\sigma}(p) a_{p\sigma} + \sum_h \phi_{i\sigma}(h) a_{h\sigma} \quad (19)$$

and the amplitudes  $\phi_{i\sigma}(p)$  and  $\phi_{i\sigma}(h)$  correspond to the eigenfunctions of Eq. (17) and the index  $p$  ( $h$ ) runs over empty (occupied) states.

$\delta F^{\text{ph}}$  contains the expansion with respect to the double-occupancy parameters and the part of the density matrix, which commutes with the total particle number. This part of the RPA problem has already been studied in detail in Refs. 14,15, where it was shown that the  $\delta D$  fluctuations can be eliminated by assuming that they adjust instantaneously to the evolution of the density matrix (antiadiabaticity condition).

Finally, the particle-particle part of the expansion reads:

$$\delta F^{\text{pp}} = \sum_{ijkl} V_{ijkl} \kappa_{ij}^* \kappa_{kl} \quad (20)$$

with  $V_{ijkl} = (V_{klji})^*$  and the matrix elements of the effective interaction are given by

$$\begin{aligned} V_{iiii} &= \sum_j t_{ij} \left\{ \left( \langle c_{j\uparrow}^\dagger c_{i\uparrow} \rangle_0 + \langle c_{i\uparrow}^\dagger c_{j\uparrow} \rangle_0 \right) A_{j++}^0 A_{i++}'' + \right. \\ &\quad \left. + \left( \langle c_{j\downarrow}^\dagger c_{i\downarrow} \rangle_0 + \langle c_{i\downarrow}^\dagger c_{j\downarrow} \rangle_0 \right) A_{j--}^0 A_{i--}'' \right\} + \frac{U}{1-n_i} \\ V_{iijj} &= -t_{ij} A_i' A_j' \left\{ \langle c_{j\uparrow}^\dagger c_{i\uparrow} \rangle_0 + \langle c_{j\downarrow}^\dagger c_{i\downarrow} \rangle_0 \right\} \text{ for } i \neq j \\ V_{ijjj} &= (V_{jjij})^* = t_{ij} A_{i++}^0 A_j' \quad \text{for } i \neq j \\ V_{ijii} &= (V_{iijj})^* = -t_{ij} A_{j--}^0 A_i' \quad \text{for } i \neq j \\ V_{ijkl} &= 0 \quad \text{otherwise.} \end{aligned}$$

Here,  $A_{i\tau\tau'}$  (with  $\tau, \tau' = \pm$ ) are the matrix elements of Eq. (10) and we have defined the following abbreviations for the derivatives:

$$A_i' = \left. \frac{\partial A_{i+-}}{\partial \langle J_i^- \rangle} \right|_0 = \left. \frac{\partial A_{i-+}}{\partial \langle J_i^+ \rangle} \right|_0, \quad (21)$$

$$A_{i\tau\tau}'' = \left. \frac{\partial^2 A_{i\tau\tau}}{\partial \langle J_i^+ \rangle \partial \langle J_i^- \rangle} \right|_0, \quad (22)$$

where explicit expressions are given in Appendix B. It is interesting to observe that, in contrast to the charge excitations in the particle-hole channel, the evaluation of the pair excitations can be performed without any assumption on the time evolution of  $\delta D$ . Only in the case

of a superconducting ground state, one would have a coupling between (ph) and (pp) fluctuations and, therefore, the necessity to invoke the antiadiabaticity condition of Refs. 14,15 to eliminate the  $\delta D$  deviations.

Note also that in contrast to HF theory (where the expansion would be given by  $U \sum_i \delta \langle J_i^+ \rangle \delta \langle J_i^- \rangle$ ), Eq. (20) contains correlations between distant pairs (i.e.,  $\delta \langle J_i^+ \rangle \delta \langle J_j^- \rangle$ ) and also processes where pairs are created and annihilated on neighboring sites (i.e.,  $\delta \langle c_{i\uparrow}^\dagger c_{j\downarrow}^\dagger \rangle$ ).

The remaining part of the formalism follows closely the particle-particle RPA as developed in nuclear physics (see Refs. 47,48). We define the  $\nu$ -th pp-RPA eigenstate of the  $N+2$  particle system by

$$|N+2, \nu\rangle = R_\nu^\dagger |N, 0\rangle, \quad (23)$$

$$R_\nu^\dagger = \sum_{p,p'} X_{pp'}^\nu a_{p\uparrow}^\dagger a_{p'\downarrow}^\dagger - \sum_{h,h'} Y_{hh'}^\nu a_{h\uparrow}^\dagger a_{h'\downarrow}^\dagger, \quad (24)$$

where  $a_{p\sigma}^\dagger$  and  $a_{h\sigma}^\dagger$  create particles and holes in the single-particle levels of the Gutzwiller Hamiltonian Eq. (17). The states  $|N, \nu\rangle$  are unprojected states in the sense of Ref. 15, i.e., they are auxiliary objects that have particle-particle RPA correlations but lack Gutzwiller correlations. This is because they result from creating particle-particle excitations on top of  $|\phi_0\rangle$  and not of  $|\Phi_G\rangle$ . In the same way, the  $\eta$ -th eigenstate of the  $N-2$  particle system can be represented as

$$|N-2, \eta\rangle = R_\eta^\dagger |N, 0\rangle, \quad (25)$$

$$R_\eta = \sum_{hh'} X_{hh'}^\eta a_{h\downarrow}^\dagger a_{h'\uparrow}^\dagger - \sum_{pp'} Y_{pp'}^\eta a_{p\downarrow}^\dagger a_{p'\uparrow}^\dagger, \quad (26)$$

where  $|N, 0\rangle$  is the unprojected RPA ground state of the  $N$ -particle system defined by

$$R_\nu |N, 0\rangle = R_\eta |N, 0\rangle = 0,$$

and we adopt the convention that  $\nu$  ( $\eta$ ) runs over the  $n_p$  ( $n_h$ ) excitations of the  $N+2$  ( $N-2$ ) particle system. Within the pp-RPA scheme  $X$  and  $Y$  amplitudes can be associated with the following unprojected matrix elements:

$$\begin{aligned} X_{pp'}^\nu &= \langle N, 0 | a_{p'\downarrow} a_{p\uparrow} | N+2, \nu \rangle, \\ Y_{hh'}^\nu &= -\langle N, 0 | a_{h\downarrow} a_{h'\uparrow} | N+2, \nu \rangle, \\ X_{hh'}^\eta &= \langle N-2, \eta | a_{h'\uparrow} a_{h\downarrow} | N, 0 \rangle, \\ Y_{pp'}^\eta &= -\langle N-2, \eta | a_{p\uparrow} a_{p'\downarrow} | N, 0 \rangle. \end{aligned}$$

From the equations of motion for the amplitudes one can derive the following eigenvalue problem<sup>47,48</sup>

$$\left( \begin{array}{c} [\xi_{p_1\downarrow} + \xi_{p_2\uparrow}] \delta_{p_1 p_3} \delta_{p_2 p_4} + V_{p_1 p_2, p_3 p_4} \\ V_{h_1 h_2, p_3 p_4}^* \end{array} \quad -[\xi_{h_1\downarrow} + \xi_{h_2\uparrow}] \delta_{h_1 h_3} \delta_{h_2 h_4} + V_{h_1 h_2, h_3 h_4} \right) \left( \begin{array}{c} W_{p_3 p_4} \\ Z_{h_3 h_4} \end{array} \right) = \left( \begin{array}{cc} I_{n_p} & 0 \\ 0 & -I_{n_h} \end{array} \right) \left( \begin{array}{c} W_{p_1 p_2} \\ Z_{h_1 h_2} \end{array} \right) \Omega^\pm, \quad (27)$$

with  $I_n$  the  $n \times n$  identity matrix. The matrix elements of the potential  $V$  can be derived from Eq. (20) by transforming to the GA representation with the help of Eq. (19).

Equations (27) yield  $n_p + n_h$  eigenvectors which can be normalized as  $|W|^2 - |Z|^2 = \pm 1$ . The sign of the norm allows one to distinguish the  $n_p$  addition eigenvectors (positive norm) from the  $n_h$  removal eigenvectors (negative norm).<sup>48</sup>

In the following, we will denote by  $E_\nu(N)$  and  $E_\eta(N)$  the  $N$ -particle energies of the Hamiltonian Eq. (1) when the  $\mu$  term is absent and write the  $\mu$  contribution explicitly, so that the eigenvalues of Eq. (1) are given by  $E_\eta(N) - \mu N$ . The eigenvalues and eigenvectors can be identified with the excitation energies and the amplitudes in the following form:

$$\begin{aligned} \Omega_\nu^+ &= E_\nu(N+2) - E_0(N) - 2\mu, & (28) \\ W_{pp'}^\nu &= X_{pp'}^\nu, \\ Z_{hh'}^\nu &= Y_{hh'}^\nu, \end{aligned}$$

for two-particle addition and

$$\begin{aligned} \Omega_\eta^- &= E_0(N) - E_\eta(N-2) - 2\mu, & (29) \\ W_{pp'}^\eta &= Y_{pp'}^\eta, \\ Z_{hh'}^\eta &= X_{hh'}^\eta, \end{aligned}$$

for two-particle removal.

Stability requires that  $\Omega_\nu^+ > 0 > \Omega_\eta^-$  thus if there exists a chemical potential  $\mu$  such that these two conditions are satisfied the system is stable, otherwise a pairing instability arises.

In a finite system, the allowed range of  $\mu$  shrinks to zero as an instability is approached. From Eqs. (28) and (29) one sees that stability requires  $E_0(N+2) - E_0(N) > E_0(N) - E_0(N-2)$ . This coincides with the stability against a transfer of a pair of particles from one cluster to another one in an ensemble. Notice that it does not necessarily coincide with the stability against single particle transfers. In the thermodynamic limit both conditions coincide with the well known stability condition that the compressibility must be positive.

We are now in the position to evaluate the pairing correlation function within the TDGA. We are interested in on-site s-wave (s) pairing and intersite pairing:

$$\Delta_i^s = c_{i\downarrow} c_{i\uparrow}, \quad (30)$$

$$\Delta_i^\delta = \frac{1}{\sqrt{2}} (c_{i+\delta\downarrow} c_{i\uparrow} + c_{i\downarrow} c_{i+\delta\uparrow}), \quad (31)$$

where  $\delta = x, y$  and  $i + \delta$  is a shorthand for the first neighbor of site  $i$  in the  $\delta$  direction.

The dynamical pairing correlations can be computed from:

$$\begin{aligned} P_{ij}^{\alpha\beta}(\omega) &= -\frac{i}{N_s} \int_{-\infty}^{\infty} dt e^{i\omega t} \langle \mathcal{T} \Delta_i^\alpha(t) [\Delta_j^\beta(0)]^\dagger \rangle & (32) \\ &= \frac{1}{N_s} \sum_\nu \frac{\langle N, 0 | \bar{\Delta}_i^\alpha | N+2, \nu \rangle \langle N+2, \nu | (\bar{\Delta}_j^\beta)^\dagger | N, 0 \rangle}{\omega - \Omega_\nu^+ + i0^+} - \frac{1}{N_s} \sum_\eta \frac{\langle N, 0 | (\bar{\Delta}_j^\beta)^\dagger | N-2, \eta \rangle \langle N-2, \eta | \bar{\Delta}_i^\alpha | N, 0 \rangle}{\omega - \Omega_\eta^- - i0^+}, \end{aligned}$$

where  $N_s$  denotes the number of sites of the system and  $\alpha = s, x, y$ . The average in the first line is done on the Gutzwiller projected RPA state. The latter is our best estimate for the true ground state of the system. The matrix elements in the second line are done on the unprojected states. In the spirit of the GA, Gutzwiller projections are effectively taken into account by a renormalization of the operators. As usual local operators do not get renormalized, i.e.,  $\bar{\Delta}_i^s \equiv \Delta_i^s$ , whereas non-local oper-

ators acquire a renormalization through the  $z$  factors:

$$\bar{\Delta}_i^\delta \equiv \frac{1}{\sqrt{2}} (z_{i+\delta\downarrow} z_{i\uparrow} c_{i+\delta\downarrow} c_{i\uparrow} + z_{i\downarrow} z_{i+\delta\uparrow} c_{i\downarrow} c_{i+\delta\uparrow}). \quad (33)$$

This is similar to the renormalization of the GA current operator in the computation of the optical conductivity.<sup>15</sup> The validity of this prescription can be checked using sum rules as discussed below. Obviously in the HF theory based on BLA, bare operators are used in Eq. (32).

The matrix elements of the pairing operators can be obtained from the amplitudes  $X$  and  $Y$  using the trans-

formation Eq. (19). In Eq. (32) the first and second term represent the correlations in case of two-particle addition and removal, respectively.

In the case of a separable potential  $V_{k_1 k_2, k_3 k_4} = v_{k_1 k_2} v_{k_3 k_4}^*$  the pp-RPA equations can be easily solved. In particular for the case of a paramagnetic solution analyzed in Ref. 38 the TDGA interaction kernel Eq. (20) only involves local pairs

$$\delta F^{\text{PP}} = V \sum_i \delta \langle c_{i\uparrow}^\dagger c_{i\downarrow}^\dagger \rangle \delta \langle c_{i\downarrow} c_{i\uparrow} \rangle \quad (34)$$

with

$$V = \frac{U - 2\Sigma_\sigma}{1 - n}, \quad (35)$$

where  $n \equiv N/N_s$  and  $\Sigma_\sigma$  is defined in Eq. (18). In this case the on-site response can be found in momentum space:

$$P_{ii}^{\alpha\alpha}(\omega) = \frac{1}{N_s} \sum_{\mathbf{q}} P_{\alpha\alpha}(\mathbf{q}, \omega) \quad (36)$$

$$P_{\alpha\alpha}(\mathbf{q}, \omega) = -\frac{i}{N_s} \int_{-\infty}^{\infty} dt e^{i\omega t} \langle \mathcal{T} \Delta_{\mathbf{q}}^\alpha(t) [\Delta_{\mathbf{q}}^\alpha(0)]^\dagger \rangle.$$

with ( $\alpha = s$ )

$$\Delta_{\mathbf{q}}^\alpha = \frac{1}{N_s} \sum_j \Delta_i^\alpha e^{i\mathbf{q} \cdot \mathbf{R}_j} \quad (37)$$

and is given by an effective ladder type equation:

$$P_{ss}(\mathbf{q}, \omega) = \frac{P_{ss}^0(\mathbf{q}, \omega)}{1 - V P_{ss}^0(\mathbf{q}, \omega)} \quad (38)$$

$$P_{ss}^0(\mathbf{q}, \omega) = \frac{1}{N_s} \sum_{\mathbf{k}} \frac{1 - f(\xi_{\mathbf{k}}) - f(\xi_{\mathbf{k}+\mathbf{q}})}{\omega - \xi_{\mathbf{k}} - \xi_{\mathbf{k}+\mathbf{q}} + i\eta_{\mathbf{k}, \mathbf{k}+\mathbf{q}}}. \quad (39)$$

with  $f(\xi_{\mathbf{k}})$  the Fermi distribution function, and  $\eta_{\mathbf{k}, \mathbf{k}'} \equiv 0^+ \text{sign}(\xi_{\mathbf{k}} + \xi_{\mathbf{k}'})$ . The single particle energies are given by  $\xi_{\mathbf{k}} = \varepsilon_{\mathbf{k}} - \mu$  where  $\varepsilon_{\mathbf{k}} \equiv z_0^2 e_{\mathbf{k}} + \Sigma_G$  is the GA dispersion relation and  $e_{\mathbf{k}} = \sum_j t_{ij} e^{-i\mathbf{k} \cdot (\mathbf{R}_j - \mathbf{R}_i)}$  is the bare one and  $z_0$  is the hopping renormalization factor Eq. (13) evaluated at the saddle point.

We are interested also in the fluctuation response for intersite bond singlets with s-wave symmetry ( $\alpha = +$ ) or d-wave ( $\alpha = -$ ) symmetry:

$$\Delta_i^\alpha = \frac{1}{2} (\Delta_i^x + \Delta_i^{-x} + \alpha \Delta_i^y + \alpha \Delta_i^{-y})$$

In this case the ladder series takes the following matrix form:

$$\underline{\underline{P}}(\mathbf{q}, \omega) = \underline{\underline{P}}^0(\mathbf{q}, \omega) + \underline{\underline{P}}^0(\mathbf{q}, \omega) \underline{\underline{\Gamma}} \underline{\underline{P}}(\mathbf{q}, \omega) \quad (40)$$

with

$$\underline{\underline{P}}(\mathbf{q}, \omega) = \begin{pmatrix} P_{ss}(\mathbf{q}, \omega) & P_{s\alpha}(\mathbf{q}, \omega) \\ P_{\alpha s}(\mathbf{q}, \omega) & P_{\alpha\alpha}(\mathbf{q}, \omega) \end{pmatrix}; \quad \underline{\underline{\Gamma}} = \begin{pmatrix} V & 0 \\ 0 & 0 \end{pmatrix}.$$

Thus

$$P_{\alpha\alpha}(\mathbf{q}, \omega) = P_{\alpha\alpha}^0(\mathbf{q}, \omega) + \frac{P_{\alpha s}^0(\mathbf{q}, \omega) V P_{s\alpha}^0(\mathbf{q}, \omega)}{1 - V P_{ss}^0(\mathbf{q}, \omega)} \quad (41)$$

and the poles of  $P_{\alpha\alpha}(\mathbf{q}, \omega)$  are determined by the local pair correlation ( $1 - V P_{ss}^0(\mathbf{q}, \omega) = 0$ ) and the bare correlation.

Eqs. (38)-(41) are also valid in the BLA approach, replacing the Gutzwiller local self-energy with the HF one ( $\Sigma_\sigma = U n/2$ ,  $z_0 = 1$ ) and taking  $V = U$ .

The exact on-site s-wave spectral density satisfies the following sum rules:

$$-\frac{1}{\pi} \int_0^\infty d\omega \text{Im} P_{ii}^{ss}(\omega) = 1 - n + \langle n_{i\uparrow} n_{i\downarrow} \rangle \quad (42)$$

$$-\frac{1}{\pi} \int_{-\infty}^0 d\omega \text{Im} P_{ii}^{ss}(\omega) = -\langle n_{i\uparrow} n_{i\downarrow} \rangle. \quad (43)$$

In our case these sum rules allow us to compute RPA corrections to the double occupancy and they will be used below to evaluate RPA corrections to the GA ground state energy. Notice that the total spectral weight is equal to  $1 - n$ .

In addition the following energy weighted sum rule is satisfied

$$M_1^{ss}(\infty) = \frac{2}{N_s} \langle T \rangle_{GA} + (2\mu - U)(1 - n) \quad (44)$$

$$M_1^{ss}(\omega) = \frac{1}{\pi N_s} \sum_{ij} \int_{-\infty}^{\omega} d\bar{\omega} \bar{\omega} \text{Im} P_{ij}^{ss}(\bar{\omega}). \quad (45)$$

with  $T$  the kinetic energy. This sum rule is satisfied exactly within the present pp-RPA in the sense that the right and the left hand side are equal, provided the kinetic expectation value on the r.h.s. is computed at the GA level. Thus in contrast with Eqs. (42) and (43) this sum rule provides no new information but is useful to perform a consistency check. The same prescription is valid in the conventional HF plus pp-RPA approach, where the r.h.s. expectation values have to be computed at HF level.<sup>49</sup> As shown in Appendix C the consistent renormalization of intersite operators can be checked from an analogous sum rule.

### III. RESULTS

In this section we present results for pair correlations in the repulsive Hubbard model within the framework developed above. Since the RPA-type scheme used in the TDGA differs in some regard from the approaches usually invoked in solid-state theory, we first illustrate the method for a two-site model which also can be solved exactly. Due to the mean-field character of the present approximations the method is expected to improve with dimensionality so this zero-dimensional example represents the worst case and allows us to give a first check of the potentialities and limitations of the method. Finally, we

compare our method with exact results on small clusters and demonstrate its superior performance as compared to the BLA.

### A. Two-site model

In order to illustrate the formalism we consider a two-site model with two particles having up and down spins. The ground-state wave function reads as

$$|2, 0\rangle = \alpha|S\rangle + \beta|D\rangle, \quad (46)$$

where

$$|S\rangle = \frac{1}{\sqrt{2}}(|1_\uparrow 2_\downarrow\rangle - |1_\downarrow 2_\uparrow\rangle), \quad (47)$$

$$|D\rangle = \frac{1}{\sqrt{2}}(|1_\uparrow 1_\downarrow\rangle + |2_\uparrow 2_\downarrow\rangle), \quad (48)$$

and the corresponding amplitudes and the ground-state energy  $E_0(2)$  are given by

$$\alpha = \frac{2t}{\sqrt{\omega_0^2 + 4t^2}}, \quad (49)$$

$$\beta = \frac{-\omega_0}{\sqrt{\omega_0^2 + 4t^2}}, \quad (50)$$

$$E_0(2) = \omega_0 \equiv \frac{U}{2} \left[ 1 - \sqrt{1 + \frac{16t^2}{U^2}} \right] \quad (51)$$

For four and zero particles there is only one state with energy  $E(4) = 2U$  and  $E(0) = 0$ , respectively. The energy differences between two-particle addition (removal) states and the ground state are

$$\Omega^+ = E(2+2) - E_0(2) - 2\mu = \frac{U}{2} + \frac{1}{2}\sqrt{U^2 + 16t^2},$$

$$\Omega^- = E_0(2) - E(2-2) - 2\mu = -\Omega^+,$$

and the chemical potential is taken as  $\mu = U/2$  which is the exact value at half filling at an infinitesimal temperature. The corresponding matrix elements for local ( $s$ ) and intersite ( $x$ ) pairing operators

$$\Delta_s = \frac{1}{\sqrt{2}}(c_{1\downarrow}c_{1\uparrow} + c_{2\downarrow}c_{2\uparrow}), \quad (52)$$

$$\Delta_x = \frac{1}{\sqrt{2}}(c_{1\downarrow}c_{2\uparrow} - c_{1\uparrow}c_{2\downarrow}), \quad (53)$$

read as

$$\langle 2, 0|\Delta_s|2+2\rangle = \langle 2, 0|\Delta_s^\dagger|2-2\rangle = \beta, \quad (54)$$

$$\langle 2, 0|\Delta_x|2+2\rangle = \langle 2, 0|\Delta_x^\dagger|2-2\rangle = \alpha. \quad (55)$$

Notice that there is only one state with  $2 \pm 2$  particles so we dropped the excitation index. One can check that the sum rules of Eq. (42)-(44) are satisfied. For example the double occupancy is given by  $\beta^2/2$  and the first moment sum rule

$$\begin{aligned} & -\frac{2}{N_s}\langle T\rangle - (2\mu - U)(1 - n) \\ & = \Omega^+|\langle 2, 0|\Delta_s|2+2\rangle|^2 - \Omega^-|\langle 2, 0|\Delta_s^\dagger|2-2\rangle|^2 \\ & = 2(U - \omega_0)\beta^2 = -\langle T\rangle \end{aligned}$$

is also fulfilled, as it should.

Consider now the same model within the TDGA. On the GA level, one finds two single particle states for each spin direction which at half filling can be put as:

$$\xi_{h\sigma} = -t(1 - u^2) + \Sigma_\sigma - \mu, \quad (56)$$

$$\xi_{p\sigma} = t(1 - u^2) + \Sigma_\sigma - \mu. \quad (57)$$

where the h-states is occupied with a spin-up and spin-down particle and we have defined  $u \equiv U/U_{BR}$  with  $U_{BR} = 8t$ . For  $U < U_{BR}$  there is a paramagnetic solution which becomes insulating at the Brinkmann-Rice transition point  $U_{BR}$ .<sup>50</sup> For  $u > \sqrt{2} - 1$  the more stable solution is an antiferromagnetic broken symmetry solution which does not have a Brinkmann-Rice transition point.

For the paramagnetic solution one has spin-independent Lagrange multipliers which from the Kotliar-Ruckenstein (or Gebhard's) scheme are obtained as

$$\Sigma_\sigma \equiv \Sigma_0 = \mu = \frac{U}{2}. \quad (58)$$

Since there is only one two-particle addition and removal state, we have to diagonalize the following  $2 \times 2$  pair fluctuation RPA problem

$$\begin{pmatrix} 2t(1 - u^2) + V/2 & V/2 \\ V/2 & 2t(1 - u^2) + V/2 \end{pmatrix} \begin{pmatrix} X \\ Y \end{pmatrix} = \Omega \begin{pmatrix} 1 & 0 \\ 0 & -1 \end{pmatrix} \begin{pmatrix} X \\ Y \end{pmatrix} \quad (59)$$

and the interaction  $V$  corresponds to the local part in

the expansion Eq. (20) (note that the first derivatives of

$A_i^0$  vanish for a paramagnetic solution)

$$V = -2t(1 - u^2)A'' + \frac{U}{1 - n} = 4tu(2 - u)\frac{1 + u}{1 - u} \quad (60)$$

where  $A''$  is defined in Appendix B. Here, the diverging part, proportional to  $1/(1 - n)$ , is canceled by an analogous contribution in the first term. The same result can be obtained from Eq. (35) by taking the limit  $n \rightarrow 1$ ,<sup>38</sup> and coincides in modulus with the effective interaction at half filling in the particle-hole case.<sup>13,14,15</sup> This is consistent with the fact that the attractive-repulsive transformation converts particle-particle fluctuations in particle hole-fluctuations with equal interaction but sign reversed.<sup>51</sup>

Diagonalization of Eq. (59) yields the two eigenvalues

$$\Omega^\pm = \pm 2t(1 - u^2)\sqrt{1 + \frac{V}{2t(1 - u^2)}}. \quad (61)$$

For the eigenvectors, the following relations hold

$$(X^\pm + Y^\pm)^2 = \pm \frac{2t(1 - u^2)}{\Omega^\pm}, \quad (62)$$

$$(X^\pm)^2 - (Y^\pm)^2 = \pm 1, \quad (63)$$

from which one can compute the amplitudes for the local and intersite pairing correlations between *unprojected* states:

$$\langle 2, 0 | \Delta_s | 2 \pm 2 \rangle = \frac{1}{\sqrt{2}}(X^\pm + Y^\pm), \quad (64)$$

$$\langle 2, 0 | \Delta_x | 2 \pm 2 \rangle = -\frac{1}{\sqrt{2}}(X^\pm - Y^\pm). \quad (65)$$

Finally, the expectation values between Gutzwiller *projected* states are the same as for unprojected states in the case of  $\Delta_s$  and should be renormalized in the intersite case, i.e.,  $\bar{\Delta}_x = (1 - u^2)\Delta_x$ . See Appendix C for a consistency check of this prescription.

For the local pairing operator we find that the first moment sum rule Eq. (44)

$$\begin{aligned} & \Omega^+ |\langle 2, 0 | \Delta_s | 2 + 2 \rangle|^2 - \Omega^- |\langle 2, 0 | \Delta_s^\dagger | 2 - 2 \rangle|^2 \\ &= 2t(1 - u^2) = -\frac{2}{N} \langle T \rangle_{GA} - 2\mu(1 - n) + U(1 - n) \end{aligned} \quad (66)$$

is satisfied (note that  $n = 1$ ) in the TDGA, as anticipated.

The TDGA two-particle addition and removal energies are displayed in Fig. 1 and compared with the exact ones. Solutions obtained in the paramagnetic regime are shown with solid lines. Remarkably, due to a cancellation of  $(1 - u)$  terms the Brinkmann-Rice transition does not reflect in the excitation energies of the paramagnetic phase, which become soft at a much larger value of the repulsion ( $u = 1 + \sqrt{2}$ ). Instead, the transition shows up in the TDGA pairing correlations (right panel of Fig. 1). Indeed, the Gutzwiller renormalization factors  $z_{i\sigma}$  drive the

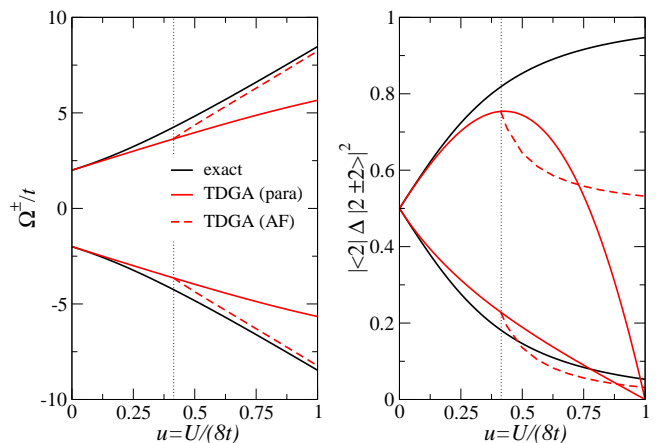


FIG. 1: (color online) Left panel: Excitation energies for two-particle addition and removal computed for the two-site model with two particles. Right panel: Matrix element of the local (lower curves) and intersite (upper curves) pairing operator. The underlying GA saddle-points are paramagnetic (p) (solid lines) and antiferromagnetic (dashed lines). The critical value  $u = \sqrt{2} - 1$  of the corresponding transition is indicated by the vertical dotted line.

matrix elements of the intersite pairing operator to zero at the Brinkmann-Rice transition point. It is interesting that neglecting  $z_{i\sigma}$  in the pairing operator, the suppression is replaced by a divergence so that the  $z_{i\sigma}$  cancel the unphysical divergence but overcorrect it. This problem is partially cured in the broken symmetry state (dashed lines) but for  $U \rightarrow \infty$  the matrix element tends to  $1/2$  whereas the exact result approaches  $|\langle 2 - 2 | \Delta_x | 2, 0 \rangle|^2 \rightarrow 1$  since the ground state can be written as  $\Delta_x^\dagger | 2 - 2 \rangle$  in this limit. Instead, the ground state with broken symmetry has only one configuration of the two that generate the singlet ground state which explains the  $1/2$  factor. For the local pairing operator the behavior is better.

We notice that the TDGA excitations energies are in quite good agreement with the exact values, especially when one allows for the broken symmetry solutions.

Finally we can use Eq. (42) to compute the pair fluctuation derived double occupancy:

$$D^{RPA} = \langle n_{i\uparrow} n_{i\downarrow} \rangle = \langle 2, 0 | c_{i\downarrow} c_{i\uparrow} | 2 + 2 \rangle \langle 2 + 2 | c_{i\uparrow}^\dagger c_{i\downarrow}^\dagger | 2, 0 \rangle. \quad (67)$$

Fig. 2 (left panel) shows the double occupancy in different approximations. HF completely neglects correlations and hence the double occupancy is independent of  $U$ . The BLA based correction drives the approximation much closer to the exact result at small  $U$  but strongly underestimates the correction at large  $U$ . In the GA, correlations are taken into account already at the static level and the double occupancy is strongly suppressed as a function of  $U$ . Thus the pp-TDGA correction is small and brings the double occupancy close to the exact one in a much larger range of interaction. The fact that the pp-TDGA is close to the GA double occupancy indicates that the theory is nearly self-consistent. In Ref. 38 it was



shown that this feature is enhanced in two-dimensions pointing to an improvement of the performance as the dimensionality is increased. In contrast the BLA is clearly quite far from being self-consistent in this sense.

For large  $U$ , the exact double occupancy is of order  $UJ \sim t^2/U^2$  due to the same charge fluctuations that build the double exchange interaction  $J$ .<sup>52</sup> Since the GA and the TDGA results in Fig. 2 are for paramagnetic solutions the double occupancy vanishes at the Brinkman-Rice point. This makes clear that the scale  $J$  is not present in the paramagnetic GA or TDGA.

The above results allow us to compute the pp-RPA ground state energy using the coupling constant integration trick<sup>53,54</sup>

$$E_0^{RPA} = -2t + UN_s \int_0^U dU' D^{RPA}(U'). \quad (68)$$

Here the first term is the ground state energy for  $U = 0$ . Restricting on the paramagnetic solutions, we find for the TDGA and BLA

$$E_0^{TDGA} = -2t + 4t(\sqrt{1 + 2u - u^2} - 1), \quad (69)$$

$$E_0^{BLA} = -2t + 2t(\sqrt{1 + U/2} - 1), \quad (70)$$

which both yield the exact result  $\omega_0$  up to second order in  $U/t$ .

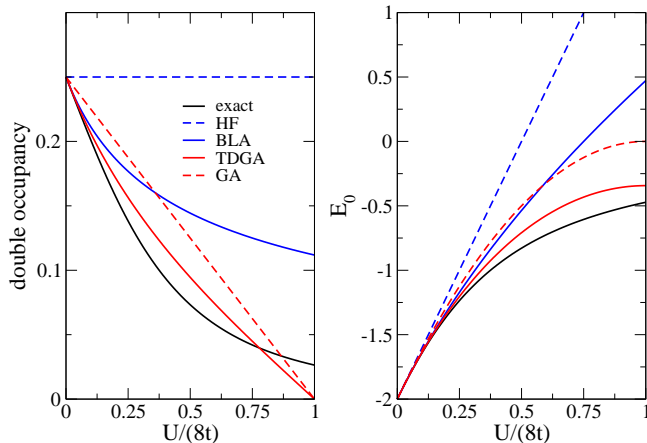


FIG. 2: (color online) Double occupancy (left panel) and ground-state energy (right panel) of the two-site Hubbard model computed within HF, BLA, TDGA, and exact diagonalization. Only paramagnetic ground states are considered.

Due to the more accurate estimate for the double occupancy (see Fig. 2a) it turns out that the TDGA gives a significantly better approximation for the ground-state energy (see Fig. 2b) than the BLA over the whole range of  $U$ , before the onset of the Brinkmann-Rice transition. This should be compared with an analogous calculation in the particle-hole channel in Ref. 15. In the latter case one obtains a singularity in  $E_0$  at  $u = 8(\sqrt{2} - 1)$  due to the onset of the antiferromagnetic ground state. Since there is no instability in the particle-particle channel,

such problems do not arise in the present case. Thus it seems convenient in general to compute RPA corrections to the energy in a channel free from instabilities.

## B. Comparison with exact diagonalization

In this section, we study the dynamical pairing correlations within the TDGA on small clusters and compare our results with the BLA approach and exact diagonalizations.

We start by computing the long-distance pairing correlations  $\langle \Delta_i^{\delta'} (\Delta_j^\delta)^\dagger \rangle$  for bond singlets. Within the pp-RPA these correlations are obtained integrating the addition part of the dynamical spectral function:

$$\langle \Delta_i^{\delta'} (\Delta_j^\delta)^\dagger \rangle = \frac{1}{\pi} \int_0^\infty d\omega \text{Im} P_{ji}^{\delta' \delta}(\omega).$$

Thus the comparison with the exact diagonalization results provides a stringent test of the total spectral weight. We remind the reader that in the TDGA the singlet operator is renormalized by the  $z_{i\sigma}$  factors.

In Fig. 3 we show results for 10 particles on a cluster with 18 sites, tilted by  $45^\circ$ , and, therefore, having all the spatial symmetries of the infinite lattice. A particular representation of this cluster, with its boundary conditions, is shown in the upper panel of Fig. 3. In this case, the GA ground state is paramagnetic. We concentrate on non-overlapping singlets and the distance between them is measured from their centers.

The two singlet operators can form a perpendicular configuration, like ‘s-b’ in the upper panel of Fig. 3, or a parallel configuration, like ‘s-a’ in the same figure. Notice that for  $R_{ij} = R_i - R_j = 2$  there are two points in the lower panel corresponding to two parallel configurations in which one of the singlets is displaced either along the x- or along the y-direction (labeled ‘a’ in the upper panel of Fig. 3).

In Fig. 3, the vertical bars point to the GA value of the singlet correlations, i.e., the decoupled result of  $\langle \Delta_i^{\delta'} (\Delta_j^\delta)^\dagger \rangle_{GA}$  but still renormalized with the  $z_{i\sigma}$  factors. In the same spirit of Ref. 22 the length and orientation of the bars reflects the ‘vertex contribution’. This quantity measures the correlation induced interaction between two singlets which is attractive when the TDGA value is larger than the one computed within the bare GA. For nearby singlets we observe excellent agreement between the exact diagonalization result and the TDGA for both  $U/t = 4$  and 10 (see lower panels of Fig. 3). In this case we also observe an effective attractive interaction. In general, with increasing distance TDGA overestimates the exact correlations, and the difference becomes more pronounced for larger  $U/t$ . This behavior can be expected due to the fact that the Gutzwiller method is based on a local projector which neglects intersite correlations. One can therefore anticipate that the incorporation of intersite projections (as in Jastrow-type wave functions<sup>55,56</sup>) into the TDGA would lead to an improvement of the

long-distance pair correlations. Nevertheless, it turns out that the TDGA yields a rather good description of long-distance pair correlations (especially for moderate values of  $U/t$ ) as compared to exact diagonalizations.

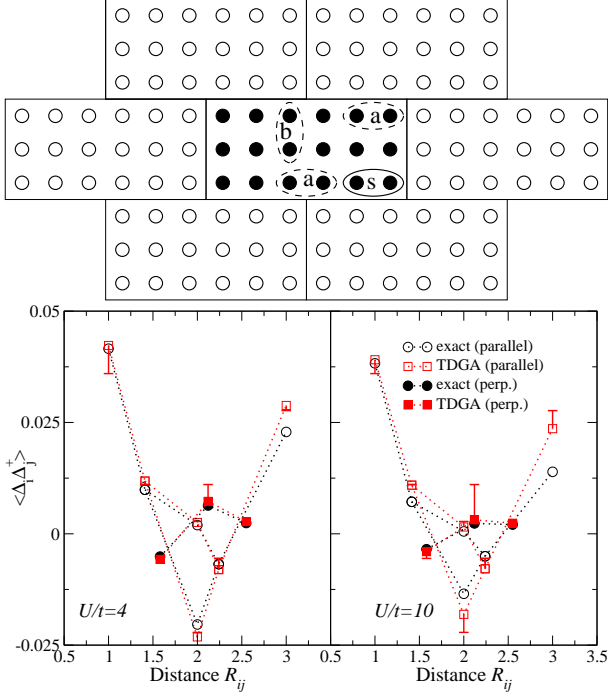


FIG. 3: (color online) Top panel: Sketch of the 18-site cluster and corresponding boundary conditions. Bottom panels: Bond singlet pairing correlations on the 18-site lattice for  $U/t = 4$  and 10. The bars at the TDGA symbols point to the bare GA value of the singlet correlations. The separation between bond singlets is defined as the shortest distance between their centers. Taking the singlet ‘s’ as reference, it should be noted that there exist two parallel singlet configurations ‘a’ with distance  $R_s - R_a = 2$ . The singlets ‘b’ and ‘s’ form a perpendicular configuration.

In order to compare dynamical properties of the TDGA with BLA and exact results, we compute the d-wave and s-wave correlations of Sec. II B. The comparison of the results in different approximations can be done by aligning the chemical potentials (as in the last figure of Ref. 38) or aligning the absolute energies. In the following, we adopt the last procedure by eliminating the chemical potential from the response function. We define  $\omega' = \omega + 2\mu$  so that the poles in  $P_{ii}^{\alpha\alpha}(\omega')$  occur at  $\omega' = E_\nu(N+2) - E_0(N)$  and  $\omega' = E_\eta(N-2) - E_0(N)$ .

In Fig. 4, we show the addition spectra for  $P_{ii}^{\alpha\alpha}(\omega')$  evaluated for a 18-site cluster with 10 particles and  $U/t = 10$ . This corresponds to a closed shell configuration where the HF and GA approach yield paramagnetic solutions. The on-site s-wave case  $P_{ii}^{ss}(\omega')$  has already been analyzed<sup>38</sup> for a smaller cluster and it is shown in Fig. 4 for 18 sites a as reference since, as explained in Sec. II B, it also determines the overall features of the intersite pairing correlations. Fig. 5 (main panel, dashed

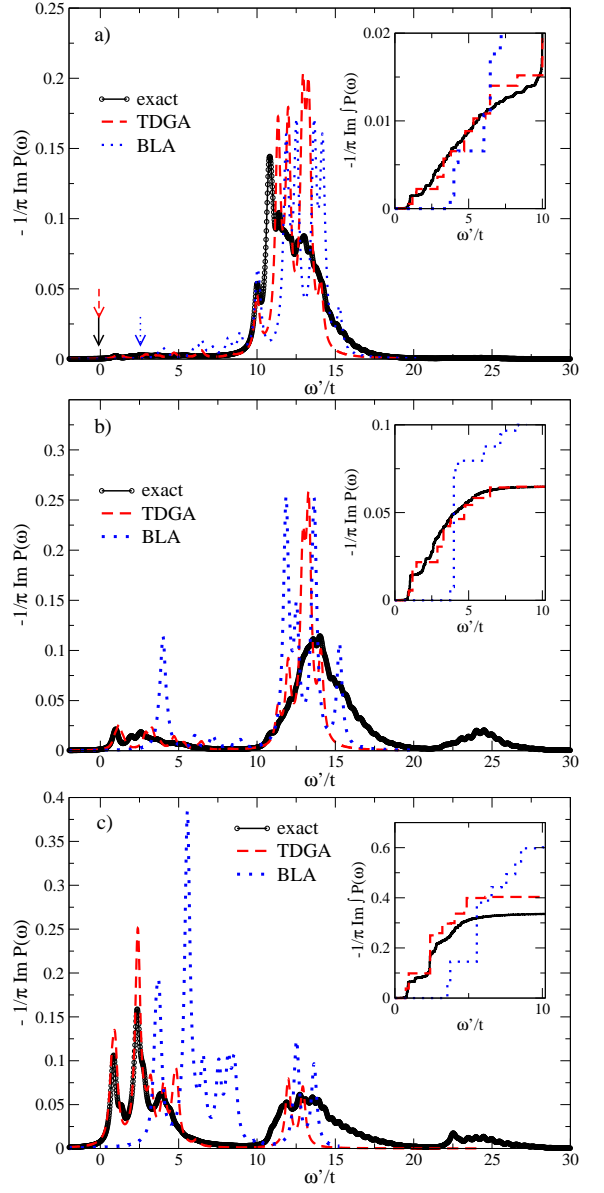


FIG. 4: (color online) Imaginary part of the (two-particle addition) pairing correlation function of Eq. (32) for on-site pairing (a), extended s-wave (b) and d-wave (c) symmetry. Results are for 10 particles on a 18-sites cluster and  $U/t = 10$  for which the underlying mean-field solution in BLA and TDGA is paramagnetic. The delta-like excitations are convoluted by lorentzians with width  $\epsilon = 0.2t$ . The arrows in the upper panel point to the chemical potentials obtained within the various methods. The insets detail the frequency evolution of the weight at small energies.

dotted line) displays the effective interaction  $V$  for the present case as a function of  $U/t$ .

In Ref. 38 we have shown that the on-site pair excitations for large  $U$  in both BLA and TDGA are dominated by an antibound which lower band edge is at  $\omega' = U$ . The band states at energies  $1t \sim 5t$  have very small spectral weight. In the top panel of Fig. 4 the full

black arrow indicates the value of  $2\mu$  in the exact case with  $\mu = (\mu^+ + \mu^-)/2$  and  $\mu^+ = E(N+1) - E(N)$ ,  $\mu^- = E(N) - E(N-1)$ . The position of  $2\mu$  in the GA (red dashed arrow) is very close to the exact one whereas in HF (blue dotted arrow) it is shifted to higher energies. Thus, aligning the chemical potentials, the position of the BLA (TDGA) antibound state is in disagreement (agreement) with the exact result.<sup>38</sup> In addition, the TDGA gives a good account of the low-energy spectral weight (see inset), which is much larger and shifted to higher energies in the BLA. This was understood as due to the different way the self-energy is renormalized by interactions in GA and in HF.<sup>38</sup> This dramatic difference in performance gets greatly amplified for intersite correlations [see Fig. 4(b) and (c)] because the band states acquire significant weight.

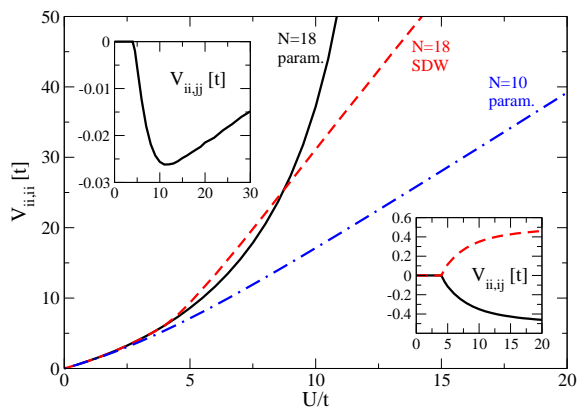


FIG. 5: (color online) Main panel: Local part of the effective interaction  $V_{ii,ii}$  (see Eq. (20)) for the 18-site cluster. The solid and dashed lines refer to the half-filled cluster with paramagnetic and spin-density wave ground state, respectively. The dashed dotted line is for the 10-particle system with a paramagnetic ground state. Upper-left inset: Effective interaction between pairs on nearest-neighbor sites  $V_{ii,jj}$ . Lower-right inset: Effective interaction  $V_{ii,ij}$  between a local pair on site  $R_i$  and an intersite pair on the bond defined by  $R_i$  and  $R_j$ .  $V_{ii,ij} > (<)0$  for  $S_i^z < (>)0$  (solid and dashed lines respectively).

The intersite correlations have also significant weight at the energy of the s-wave antibound state  $\omega' \sim U$ . This can be understood from the second term of Eq. (41) and corresponds to processes in which an intersite pair decays into an on-site pair. Notice that the d-wave pair cannot mix with a local s-wave pair at  $\mathbf{q} = \mathbf{0}$  but couples at finite  $\mathbf{q}$ .

In addition, the exact result shows a satellite at  $\omega' \approx 2U$  for the intersite cases corresponding to a process in which the two particles are created at neighboring sites, that are initially single occupied, thus leading to two on-site pairs in the final state. This can be visualized as the creation of the two particles in the upper Hubbard band. Since this band is not present in our starting point (i.e., GA), this satellite is absent in the pp-RPA. This feature reappears if one starts from a GA state that has both

lower and upper Hubbard bands at the cost of spontaneous symmetry breaking. This case is analyzed in the following.

We now consider the half-filled system where both HF and GA have a spin-density wave (SDW) ground state. The dynamical pairing correlations, for 18 particles in the 18-site cluster, are shown in Fig. 6. Again, we are comparing absolute energies, but the position of  $2\mu$  in the different approximations is aligned because the chemical potentials coincide and are equal to the exact result  $\mu = U/2$ .

For local s-wave, extended s-wave, and d-wave fluctuations the exact result has a broad distribution of weight centered around  $\omega' \sim 2U$ . Clearly this corresponds to the high-energy satellite of the previous case. Now practically all sites are singly occupied so the probability to find an empty site where to create a local s-wave pair is very small and there is practically no weight at the energy of the antibound state  $\omega' \sim U$ . Indeed, if the TDGA computation is done with a paramagnetic state (which cannot reproduce the satellite at  $2U$ ) the response becomes identically zero.<sup>38</sup> This can be also seen from the sum rule of Eqs. (42), (43) since in the paramagnetic TDGA and GA the double occupancy vanishes for the half-filled system above the Brinkman-Rice transition point.

Breaking the symmetry and allowing for the SDW, both BLA and TDGA give a good estimate of the energy scale but with a more narrow distribution of weight. Notice that the on-site s-wave response has a much smaller intensity consistent with the fact that the feature originates from intersite excitations which get mixed with the on-site response.

Processes in which the two particles are created on different singly occupied sites are allowed in both approximate theories and they lead to approximately similar results. In this case the interaction is practically ineffective. In fact, the excitation spectra evaluated from  $P^0$  (from the bare Gutzwiller Hamiltonian) shown with thin lines in Fig. 6 differ only slightly from the TDGA result and the latter only shows a small shift of spectral weight to higher energies due to the inclusion of particle-particle correlations. This is in contrast to the paramagnetic case away from half filling (see Fig. 4) where all high-energy (antibound) states are determined from poles in  $P(\omega')$  but are absent in the non-interacting case  $P^0(\omega')$  as discussed before.

The insets of Fig. 6 show the evolution of the two-particle spectral weight. For both extended s-wave and d-wave symmetry the total weight approaches  $1/2$  in the pp-RPA theories in the limit  $U \rightarrow \infty$  as for the AF solution of the two-site model in the right panel of Fig. 1. This can be easily understood from the Neel limit. In contrast, the exact result has a larger weight which can be understood from quantum fluctuations that induce spin flips. In the extreme case of the two site model, the fluctuations lead to a local singlet and the exact spectral weight for  $U \rightarrow \infty$  is twice the approximate one as dis-

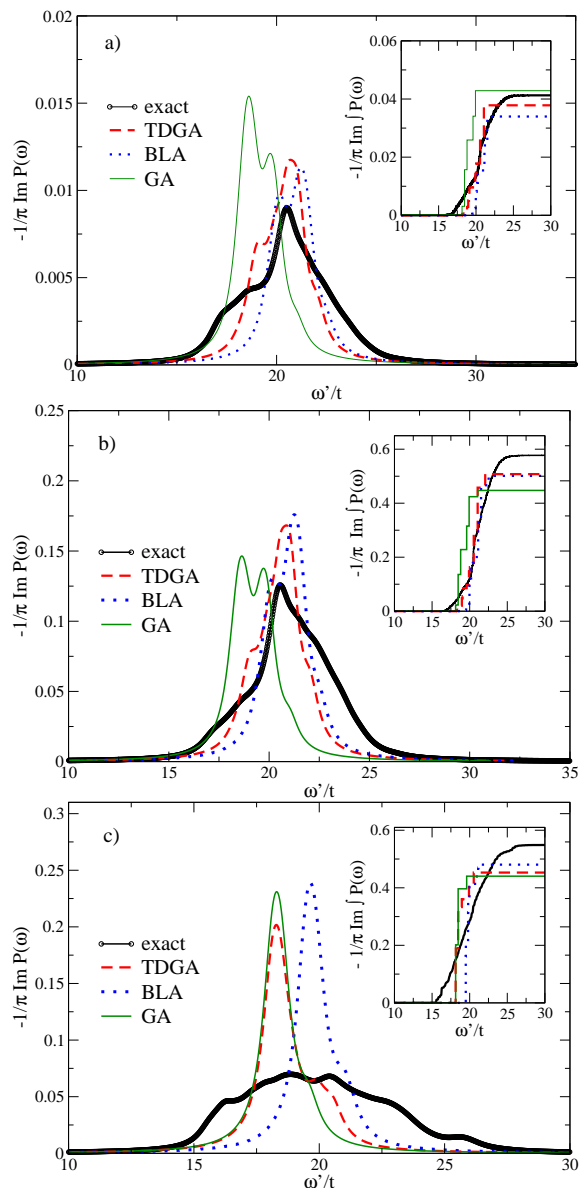


FIG. 6: (color online) Imaginary part of the (two-particle addition) pairing correlation function Eq. (32) for on-site pairing (a), extended s-wave (b) and d-wave (c) symmetry. Results are for a half-filled 18-site cluster and  $U/t = 10$ . The underlying mean-field solution in BLA and TDGA is a spin-density wave. The delta-like excitations are convoluted by lorentzians with width  $\epsilon = 0.5t$ . The insets detail the frequency evolution of the two-particle spectral weight.

cussed in connection with Fig. 1. Clearly this result is closely related to the reduction of the magnetization in a quantum antiferromagnet.

The structure of the TDGA interaction kernel Eq. (20) is more complex than the paramagnetic case. Fig. 5 displays the corresponding non-vanishing elements as a function of  $U/t$ . For small on-site repulsion the local contribution behaves as  $V_{ii,ii} \approx U$ , independent of the filling and the ground state, as it should. With the onset of the

SDW at  $U/t \approx 4.1$ ,  $V_{ii,ii}$  (dashed line) starts to deviate from the corresponding interaction in the paramagnetic limit (full line) which diverges at the Brinkmann-Rice transition.<sup>38</sup> Interestingly, the interaction between local pairs on adjacent sites (upper left inset of Fig. 5) is always attractive in the SDW phase with a maximum attraction at  $U/t \approx 10$ . In addition one finds an attractive or repulsive interaction between a local pair on site  $i$  and an intersite pair  $c_{i,\uparrow}c_{j,\downarrow}$ . For  $i$  and  $j$  nearest neighbors the interaction is attractive (repulsive) if the pair has the same (opposite) spin with respect to the underlying Neel magnetic moments of sites  $i$  and  $j$ . Nevertheless, these additional fluctuations in the TDGA cannot overcome the strong residual on-site repulsion so that the system remains stable against a transition towards superconductivity. This also holds for a SDW ground state away from half filling.

Finally, as in the two-site example, we calculate the energy correction from the TDGA for a half filled  $4 \times 4$  cluster from Eqs. (42) and (68). In Fig. 7, we compare the corresponding result for the particle-particle and particle-hole channel (from Ref. 14) with the bare GA and the exact ground-state energy. The underlying saddle-point of the GA solution is a SDW. As can be seen from Fig. 7, the particle-hole TDGA correction is approximately twice that in the particle-particle channel. The former gives a quite accurate approximation for intermediate values of the on-site repulsion but tends to overshoot the exact result for large  $U/t$  (note that these energy corrections are not derived from a variational principle and thus do not constitute an upper bound for the exact result). With the considered range of  $U/t$  the particle-particle corrections always are slightly higher in energy than the exact ground state. However, in comparison with the HF+RPA energy corrections which are by far too large,<sup>14</sup> the TDGA yields a reasonable approximation to  $E_0$  in both particle-hole and particle-particle channel.

#### IV. CONCLUSIONS

In this paper, we have extended the TDGA towards the inclusion of pair correlations in the Hubbard model. The present analysis is complementary to previous computations in the particle-hole channel<sup>14,15,16</sup> where we have analyzed the spectrum of charge- and spin excitations. In comparison with exact diagonalization results the TDGA yields a very good agreement for the dynamical pair correlation function, especially for the low-energy excitations and away from half filling where it performs significantly better than the HF based BLA theory.

Compared to numerical methods<sup>57</sup> our approach can be pushed to much larger systems. In particular, it is suitable for the evaluation of pair correlations in the negative- $U$  Hubbard model, where the approach is at least qualitatively capable to capture the crossover from weak coupling BCS to strong coupling behavior.<sup>58</sup> An important outcome of this investigation concerns the jus-

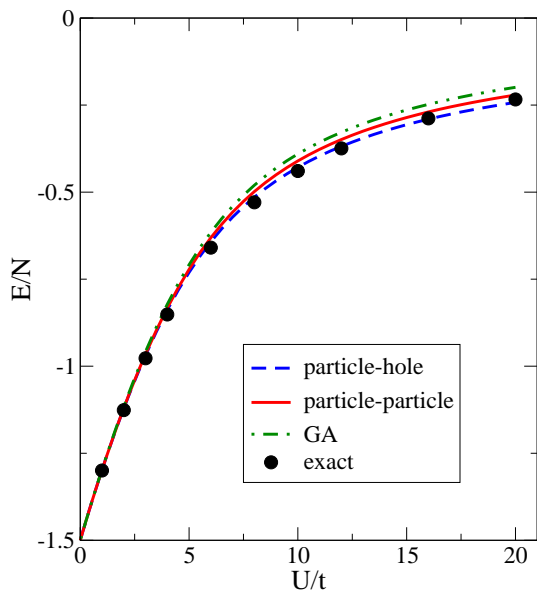


FIG. 7: (color online) Ground state energy of the half-filled  $4 \times 4$  Hubbard model computed within GA, TDGA in the particle-hole channel, TDGA in the particle-particle channel, and exact diagonalization.

tification of the antiadiabatic assumption for the time-evolution of the double occupancy, which was needed in the charge particle-hole channel.

For the Hubbard Hamiltonian with particle-hole symmetry (e.g., nearest-neighbor hopping at half filling), the superconducting instability and the charge-density wave instability in the particle-hole channel are degenerate. Evaluation of the latter instability within the TDGA requires to invoke the antiadiabaticity condition whereas the expansion in the particle-particle channel of Eq. (20) goes without it. The fact that the two calculations within the TDGA for the particle-hole and the particle-particle sector give the correct degeneracy of the instabilities for a charge-rotational invariant system clearly indicates that the antiadiabaticity assumption was indeed correct, i.e., other possibilities, as keeping the double occupancy fixed at the stationary value (rather than to follow the time evolution of the density matrix), would have led to an unphysical breaking of charge-rotational symmetry.

Our approach does not produce a superconducting instability in the Hubbard model. This is because, in the paramagnetic phase, the effective interaction does not contain the attractive part due to the exchange of spin fluctuations. Indeed, the superexchange scale  $J$  is absent in the paramagnetic GA. On the other hand, it turned out that the effective interaction in the SDW phase contained attractive contributions between nearest-neighbor pairs which, however, are too weak in order to yield a superconducting instability once the SDW is present.

The flexibility of the present approach allows one to study collective modes in inhomogeneous superconducting states once the Hamiltonian is augmented with a suit-

able pairing potential. This may find application in the physics of high- $T_c$  cuprates, where in many compounds the occurrence of electronic inhomogeneities (e.g., in the form of stripes) is now well established. Another possible application is in the field of ultra-cold atoms where the ground state is intrinsically inhomogeneous due to the presence of the confining parabolic potential. In addition, recent studies incorporate disorder to produce a glassy state, which may lead to similar physics as in the cuprates.<sup>59</sup>

### Acknowledgments

G.S. acknowledges financial support from the Deutsche Forschungsgemeinschaft. F.B. and J.L. partial support by CNR-INFN.

### APPENDIX A: DERIVATION OF THE CHARGE-ROTATIONALLY INVARIANT GA WITHIN THE SLAVE-BOSON APPROACH

The procedure implemented in the following essentially consists of three steps. Assume that in our initial reference frame we have non-vanishing superconducting order, i.e.,  $\langle J_i^+ \rangle \neq 0$  and (or) in  $\langle J_i^- \rangle \neq 0$ . First, we rotate them locally to a new frame where these expectation values vanish, i.e.,  $\langle \tilde{J}_i^+ \rangle = \langle \tilde{J}_i^- \rangle = 0$ . This allows, as a second step, the introduction of slave-bosons and associated fermions  $\tilde{f}_{i\sigma}$  within the Kotliar-Ruckenstein scheme. For the bosons, we apply the saddle-point (mean-field) approximation. Finally, in a third step, we rotate the fermions back to the original reference frame.

We define the local rotations in charge space by the following transformations

$$\tilde{\Psi}_i = \mathbf{U}_i^\dagger \Psi_i \quad \tilde{\Psi}_i^\dagger = \Psi_i^\dagger \mathbf{U}_i, \quad (\text{A1})$$

where

$$\mathbf{U}_i = \cos(\varphi_i/2) \mathbf{1} + \imath \sin(\varphi_i/2) \vec{\tau} \cdot \vec{\eta}, \quad (\text{A2})$$

and  $\vec{\eta} = (\eta_x, \eta_y, 0)$  is the rotation axis of length unity. The inverse transformation reads as

$$\Psi_i = \mathbf{U}_i \tilde{\Psi}_i \quad \Psi_i^\dagger = \tilde{\Psi}_i^\dagger \mathbf{U}_i^\dagger. \quad (\text{A3})$$

Within the first step of our procedure we have the requirement that the transformed pseudospin vector is given by  $\vec{J}_i = (0, 0, \tilde{J}_i^z)$ . Applying the transformation of Eq. (A3) to this vector one obtains the following relations

$$J_i^x = -\eta_y \sin(\varphi_i) \tilde{J}_i^z, \quad (\text{A4})$$

$$J_i^y = \eta_x \sin(\varphi_i) \tilde{J}_i^z, \quad (\text{A5})$$

$$J_i^z = \cos(\varphi_i) \tilde{J}_i^z. \quad (\text{A6})$$

Note that the spin operator

$$S_i^z = \frac{1}{2} (\Psi_i^\dagger \Psi_i - 1) = \tilde{S}_i^z \quad (\text{A7})$$

is unchanged by the transformation.

Since by definition off-diagonal order vanishes in the rotated frame we can now, as a second step, apply the Kotliar-Ruckenstein slave-boson scheme:

$$\tilde{c}_{i\sigma} = z_{i\sigma} \tilde{f}_{i\sigma} \quad \tilde{c}_{i\sigma}^\dagger = z_{i\sigma}^\dagger \tilde{f}_{i\sigma}^\dagger, \quad (\text{A8})$$

with

$$z_{i\sigma} = \frac{1}{\sqrt{e_i^\dagger e_i + p_{i,-\sigma}^\dagger p_{i,-\sigma}}} \left[ e_i^\dagger p_{i\sigma} + p_{i,-\sigma}^\dagger d_i \right] \frac{1}{\sqrt{d_i^\dagger d_i + p_{i,\sigma}^\dagger p_{i,\sigma}}}. \quad (\text{A9})$$

The double ( $d$ ), singly ( $p_\sigma$ ), and empty ( $e_i$ ) occupancy bosons are constrained by the following relations:

$$\sum_\sigma p_{i,\sigma}^\dagger p_{i,\sigma} + 2d_i^\dagger d_i = 2\tilde{J}_i^z + 1, \quad (\text{A10})$$

$$p_{i,\uparrow}^\dagger p_{i,\uparrow} - p_{i,\downarrow}^\dagger p_{i,\downarrow} = 2\tilde{S}_i^z = 2S_i^z, \quad (\text{A11})$$

$$d_i^\dagger d_i + \sum_\sigma p_{i,\sigma}^\dagger p_{i,\sigma} + e_i^\dagger e_i = 1. \quad (\text{A12})$$

Since we follow essentially a Gutzwiller-type approach, we now apply the mean-field approximation for the bosons. With the help of Eqs. (A6), (A10), (A11) and (A12) we can eliminate all bosons but  $d_i$  and express them via expectation values in the *original* reference frame and  $d_i^2$ . One finds

$$e_i^2 = -\frac{2}{\cos(\varphi_i)} \langle J_i^z \rangle + d_i^2, \quad (\text{A13})$$

$$p_{i\sigma}^2 = \frac{1}{2} + \frac{1}{\cos(\varphi_i)} \langle J_i^z \rangle + \sigma \langle S_i^z \rangle - d_i^2, \quad (\text{A14})$$

and  $\sigma \equiv \pm 1$  in the latter equation.

Summarizing the steps we have performed so far the original fermion operators  $c_{i\sigma}$  are related to the Kotliar-Ruckenstein transformed ones  $\tilde{f}_{i\sigma}$  in the rotated frame via the transformation

$$\Psi_i = \begin{pmatrix} c_{i\uparrow} \\ c_{i\downarrow} \end{pmatrix} = \mathbf{W} \begin{pmatrix} \tilde{f}_{i\uparrow} \\ \tilde{f}_{i\downarrow} \end{pmatrix}, \quad (\text{A15})$$

with

$$\mathbf{W} = \begin{pmatrix} z_{i,\uparrow} \cos \frac{\varphi_i}{2} & i(\eta_x - i\eta_y) \sin \frac{\varphi_i}{2} z_{i,\downarrow} \\ i(\eta_x + i\eta_y) \sin \frac{\varphi_i}{2} z_{i,\uparrow} & z_{i,\downarrow} \cos \frac{\varphi_i}{2} \end{pmatrix}. \quad (\text{A16})$$

Finally we transform the fermion operators  $\tilde{f}_{i\sigma}$  back to the original frame [see Eq. (A1)]

$$\begin{pmatrix} \tilde{f}_{i\uparrow} \\ \tilde{f}_{i\downarrow} \end{pmatrix} = \mathbf{U} \begin{pmatrix} f_{i\uparrow} \\ f_{i\downarrow} \end{pmatrix}, \quad (\text{A17})$$

so that the charge-rotational invariant Gutzwiller representation of the fermions is given by

$$\Phi_i = \begin{pmatrix} f_{i\uparrow} \\ f_{i\downarrow} \end{pmatrix} = \mathbf{WU} \begin{pmatrix} \tilde{f}_{i\uparrow} \\ \tilde{f}_{i\downarrow} \end{pmatrix}. \quad (\text{A18})$$

The complete transformation matrix  $\mathbf{A} = \mathbf{WU}$  reads as:

$$\mathbf{A}_i = \begin{pmatrix} z_{i\uparrow} \cos^2 \frac{\varphi_i}{2} + z_{i\downarrow} \sin^2 \frac{\varphi_i}{2} & \frac{\langle J_i^- \rangle}{2\langle J_i^z \rangle} [z_{i\uparrow} - z_{i\downarrow}] \cos \varphi_i \\ \frac{\langle J_i^+ \rangle}{2\langle J_i^z \rangle} [z_{i\uparrow} - z_{i\downarrow}] \cos \varphi_i & z_{i\uparrow} \sin^2 \frac{\varphi_i}{2} + z_{i\downarrow} \cos^2 \frac{\varphi_i}{2} \end{pmatrix}, \quad (\text{A19})$$

with

$$\tan^2 \varphi_i = \frac{\langle J_i^+ \rangle \langle J_i^- \rangle}{\langle J_i^z \rangle^2}, \quad (\text{A20})$$

and  $J_i^+$ ,  $J_i^-$  and  $J_i^z$  are defined as in Eqs. (7), (8), and (9) but with the pseudofermion operators  $f_{i\sigma}$  instead of  $c_{i\sigma}$ .

Note the formal similarity of Eq. (10) with the corresponding transformation of the spin-rotation invariant Gutzwiller approximation.<sup>16</sup>

We now turn to the transformation of the interaction term of the Hubbard Hamiltonian which has to be performed within the second step of the above scheme but *before* the saddle-point approximation has been applied to the bosons. Rewriting the interaction in terms of the transformation Eq. (A15) and obeying the constraints Eqs. (A10)-(A12) we obtain

$$n_{i\uparrow} n_{i\downarrow} = \cos^2 \frac{\varphi_i}{2} d_i^\dagger d_i + \sin^2 \frac{\varphi_i}{2} e_i^\dagger e_i, \quad (\text{A21})$$

which now can be again treated in the mean-field approximation.

We finally obtain for the charge-rotational invariant Gutzwiller energy functional of the Hubbard model

$$E = \sum_{i,j} t_{ij} \langle \Phi_i^\dagger \mathbf{A}_i \tau_z \mathbf{A}_j \Phi_j \rangle + U \sum_i \left[ d_i^2 - J_i^z (\sqrt{1 + \tan^2 \varphi_i} - 1) \right]. \quad (\text{A22})$$

The term multiplying  $U$  is clearly the sum of the double occupancies  $D_i$  of the original hamiltonian. Therefore, we perform the substitution

$$D_i = d_i^2 - J_i^z (\sqrt{1 + \tan^2 \varphi_i} - 1) \quad (\text{A23})$$

to reach Eq. (3). With this definition it is also straightforward to proof the equivalence of the saddle-point z-factors Eq. (A9) with the Gutzwiller renormalization factors  $z_{i\sigma}$  from Eq. (11) and of the two representations of the transformation matrix  $\mathbf{A}$  in Eq. (10) and Eq. (A19).

## APPENDIX B: DERIVATIVES OF THE HOPPING FACTOR

The derivatives appearing in Eqs. (21) and (22) are given by:

$$A'_i = \frac{\partial A_{i+-}}{\partial \langle J_i^- \rangle} \Big|_0 = \frac{\partial A_{i-+}}{\partial \langle J_i^+ \rangle} \Big|_0 = \frac{z_{i\uparrow} - z_{i\downarrow}}{2J_i^z} \quad (\text{B1})$$

$$A''_{i\tau\tau} = \frac{\partial^2 A_{i\tau\tau}}{\partial \langle J_i^+ \rangle \partial \langle J_i^- \rangle} \Big|_0 = -\sigma \frac{z_{i\uparrow} - z_{i\downarrow}}{(1-n_i)^2} + \frac{z_{i\tau}}{n_i - 1} \frac{n_{i\tau} - \frac{1}{2}}{n_{i\tau}(1-n_{i\tau})} \quad (\text{B2})$$

$$+ \frac{1}{1-n_i} \frac{1}{\sqrt{n_{i\tau}(1-n_{i\tau})}} \left\{ \sqrt{\frac{n_{i\tau} - D_i}{1-n_i + D_i}} - \frac{1}{2} \sqrt{\frac{1-n_i + D_i}{n_{i\tau} - D_i}} - \frac{1}{2} \sqrt{\frac{D_i}{n_{i,-\tau} - D_i}} \right\}. \quad (\text{B3})$$

Notice that the index  $\tau$  for the matrix element of  $\mathbf{A}$  appears at the place of the spin index on the right. In this case one should interpret  $+ = \uparrow$  and  $- = \downarrow$ .

In case of a homogeneous, paramagnetic saddle point these expressions simplify to

$$A'_i = 0 \quad (\text{B4})$$

$$A''_{i\tau\tau} = \frac{2z_0}{n(2-n)} + \frac{z_0}{1-n} \left[ \frac{1}{1-n+D+\sqrt{D(1-n+D)}} - \frac{1}{n-2D} \right] \quad (\text{B5})$$

where  $z_0$  denotes the spatially homogeneous Gutzwiller factor defined in Eq. (13).

### APPENDIX C: SUM RULE FOR INTERSITE PAIRING OPERATORS

We define local and extended s-wave pairing operators on a hypercubic lattice (coordination number  $\mathcal{Z}$ ) as

$$\begin{aligned} \Delta_i^s &= c_{i\downarrow} c_{i\uparrow} \\ \Delta_i^{es} &= \sum_j \gamma_{ij} [c_{i\downarrow} c_{j\uparrow} + c_{j\downarrow} c_{i\uparrow}] \end{aligned}$$

where  $\gamma_{ij} = 1$  for  $ij$  nearest neighbors and  $\gamma_{ij} = 0$  otherwise. We consider the Hubbard model Eq. (1) with nearest-neighbor hopping only. The kinetic energy operator can then be represented as

$$T = -t \sum_{ij\sigma} \gamma_{ij} c_{i\sigma}^\dagger c_{j\sigma} \quad (\text{C1})$$

and the commutator of  $\Delta_i^l$  with  $H$  yields

$$[H, \Delta_i^l] = t \Delta_i^{es} - U \Delta_i^l. \quad (\text{C2})$$

For the double-commutator with  $(\Delta_i^{es})^\dagger$  we obtain

$$\begin{aligned} & [(\Delta_i^{es})^\dagger, [H, \Delta_i^l]] = -2\mathcal{Z}t + \mathcal{Z}t(n_{i\uparrow} + n_{i\downarrow}) \\ & + t \sum_{nm} \gamma_{in} \gamma_{im} [c_{n\uparrow}^\dagger c_{m\uparrow} + c_{n\downarrow}^\dagger c_{m\downarrow}] \\ & - U \sum_n \gamma_{in} [c_{n\uparrow}^\dagger c_{i\uparrow} + c_{n\downarrow}^\dagger c_{i\downarrow}] \end{aligned} \quad (\text{C3})$$

which only depends on one-particle operators.

Taking the expectation value of Eq. (C3) and inserting a complete set of  $N+2$  and  $N-2$  particle states we find

the following sum rule

$$\begin{aligned} & \sum_i \langle [(\Delta_i^{es})^\dagger, [H, \Delta_i^l]] \rangle \\ & = \sum_{i,\nu} \omega_\nu^+ \langle \Psi_0^N | \Delta_i^l | \Psi_\nu^{N+2} \rangle \langle \Psi_\nu^{N+2} | (\Delta_i^{es})^\dagger | \Psi_0^N \rangle \\ & - \sum_{i,\nu} \omega_\nu^- \langle \Psi_0^N | (\Delta_i^{es})^\dagger | \Psi_\nu^{N-2} \rangle \langle \Psi_\nu^{N-2} | \Delta_i^l | \Psi_0^N \rangle \\ & = -2N_L \mathcal{Z}t (1 - \langle n \rangle) + \frac{U}{t} \langle T \rangle \\ & + t \sum_{in \neq m} \gamma_{in} \gamma_{im} \langle [c_{n\uparrow}^\dagger c_{m\uparrow} + c_{n\downarrow}^\dagger c_{m\downarrow}] \rangle \end{aligned} \quad (\text{C4})$$

where  $N_L$  denotes the number of lattice sites,  $\langle n \rangle$  the particle density and  $\omega_\nu^\pm = \pm [E_\nu(N \pm 2) - E_0(N)]$ .

In case of the time-dependent GA the states  $|\Psi_\nu^{N \pm 2}\rangle$  are interpreted as Gutzwiller projected RPA states, i.e. they incorporate Gutzwiller and particle-particle correlations. In the spirit of the GA matrix elements are evaluated in term of the unprojected RPA states as

$$\langle \Psi_0^N | (\Delta_i^{es})^\dagger | \Psi_\nu^{N-2} \rangle = \langle 0, N | (\bar{\Delta}_i^{es})^\dagger | \nu, N-2 \rangle$$

where  $\bar{\Delta}_i^{es}$  is renormalized with the  $z$  factors as in Eq. (33). As in HF+RPA theories one expect that the r.h.s is equal to the l.h.s when evaluated at the static mean field level in this case the GA. Indeed evaluating the kinetic expectation values on the GA approximation (incorporating the  $z$  factors) one finds and identity as expected.

We can explicitly demonstrate the procedure for the half-filled two-site model where local and intersite pairing operators are defined in Eqs. (52) and (53). For this

special case the sum rule Eq. (C4) becomes

$$\begin{aligned} \langle [(\Delta^{es})^\dagger, [H, \Delta^l]] \rangle &= \omega^+ \langle \Psi_0^2 | \Delta^l | \Psi^{2+2} \rangle \langle \Psi^{2+2} | (\Delta^{es})^\dagger | \Psi_0^2 \rangle \\ &\quad - \omega^- \langle \Psi_0^2 | (\Delta^{es})^\dagger | \Psi^{2-2} \rangle \langle \Psi^{2-2} | \Delta^l | \Psi_0^2 \rangle \\ &= \frac{U}{2t} \langle T \rangle. \end{aligned} \quad (\text{C5})$$

For the l.h.s. of Eq. (C5) we find from Eqs. (64), and (65)

$$\begin{aligned} &\omega^+ \langle 0, 2 | \Delta^l | 2 + 2 \rangle \langle 2 + 2 | (\Delta^{es})^\dagger | 0, 2 \rangle \\ &- \omega^- \langle 0, 2 | (\Delta^{es})^\dagger | 2 - 2 \rangle \langle 2 - 2 | \Delta^l | 0, 2 \rangle \\ &= -\frac{1}{2} \omega^+ [(X^+)^2 - (Y^+)^2] + \frac{1}{2} \omega^- [(X^-)^2 - (Y^-)^2] \\ &= -\frac{1}{2} [\omega^+ + \omega^-] = -2\Sigma_0 = -U. \end{aligned} \quad (\text{C6})$$

Evaluating the r.h.s. of Eq. (C5) within the GA one obtains

$$\frac{U}{2t} \langle T \rangle_{GA} = \frac{U}{2t} (-2t)(1 - u^2) = -U(1 - u^2) \quad (\text{C7})$$

so that in the time-dependent GA the intersite pairing operator Eq. (53) has to be renormalized according to

$$\bar{\Delta}_x = \frac{1}{\sqrt{2}} (1 - u^2) (c_{1\downarrow} c_{2\uparrow} - c_{1\uparrow} c_{2\downarrow}) \quad (\text{C8})$$

in order to fulfill the sum rule Eq. (C5).

- 
- <sup>1</sup> M.C. Gutzwiller, Phys. Rev. Lett. **10**, 159 (1963).  
<sup>2</sup> G. Baskaran, Z. Zou, and P.W. Anderson, Solid State Commun. **63**, 973 (1987).  
<sup>3</sup> G. Kotliar and J. Liu, Phys. Rev. B **38**, 5142 (1988).  
<sup>4</sup> A. Paramekanti, M. Randeria, and N. Trivedi, Phys. Rev. Lett. **87**, 217002 (2001).  
<sup>5</sup> S. Sorella, G.B. Martins, F. Becca, C. Gazza, L. Capriotti, A. Parola, and E. Dagotto, Phys. Rev. Lett. **88**, 117002 (2002).  
<sup>6</sup> W. Metzner and D. Vollhardt, Phys. Rev. Lett. **59**, 121 (1987).  
<sup>7</sup> W. Metzner and D. Vollhardt, Phys. Rev. B **37**, 7382 (1988).  
<sup>8</sup> F. Gebhard, Phys. Rev. B **41**, 9452 (1990).  
<sup>9</sup> M.C. Gutzwiller, Phys. Rev. **134**, A 923 (1964); *ibid.* **137**, A 1726 (1965).  
<sup>10</sup> G. Kotliar and A.E. Ruckenstein, Phys. Rev. Lett. **57**, 1362 (1986).  
<sup>11</sup> J. Lorenzana and G. Seibold, Phys. Rev. Lett. **89**, 136401 (2002).  
<sup>12</sup> J. Bünemann, F. Gebhard, T. Ohm, S. Weiser, and W. Weber, in *Frontiers in Magnetic Materials*, ed. A. Narlikar, Springer (2005).  
<sup>13</sup> D. Vollhardt, Rev. Mod. Phys. **56**, 99 (1984).  
<sup>14</sup> G. Seibold and J. Lorenzana, Phys. Rev. Lett. **86**, 2605 (2001).  
<sup>15</sup> G. Seibold, F. Becca, and J. Lorenzana, Phys. Rev. B **67**, 085108 (2003).  
<sup>16</sup> G. Seibold, P. Rubin, F. Becca, and J. Lorenzana, Phys. Rev. B **69**, 155113 (2004).  
<sup>17</sup> J. Lorenzana and G. Seibold, Phys. Rev. Lett. **90**, 066404 (2003).  
<sup>18</sup> G. Seibold and J. Lorenzana, Phys. Rev. Lett. **94**, 107006 (2005).  
<sup>19</sup> G. Seibold and J. Lorenzana, Phys. Rev. B **73**, 144515 (2006).  
<sup>20</sup> E. Dagotto, J. Riera, and A. P. Young, Phys. Rev. B **42**, 2347 (1990).  
<sup>21</sup> F. Becca, A. Parola, and S. Sorella, Phys. Rev. B **61**, 16287(R) (2000).  
<sup>22</sup> S.R. White, D.J. Scalapino, R.L. Sugar, N.E. Bickers, and R.T. Scalettar, Phys. Rev. B **39**, R839 (1989).  
<sup>23</sup> A. Moreo, Phys. Rev. B **45**, 5059 (1992).  
<sup>24</sup> N. Bulut, D.J. Scalapino, and S.R. White, Phys. Rev. B **47**, 14599 (1993).  
<sup>25</sup> S. Zhang, J. Carlson, and J.E. Gubernatis, Phys. Rev. Lett. **78**, 4486 (1997).  
<sup>26</sup> E. Plekhanov, F. Becca, and S. Sorella, Phys. Rev. B **71**, 064511 (2005).  
<sup>27</sup> R. Arita and K. Held, Phys. Rev. B **73**, 064515 (2006).  
<sup>28</sup> T. Yanagisawa, Phys. Rev. B **75**, 224503 (2007).  
<sup>29</sup> R.A. Ferrell, J. Low Temp. Phys. **1**, 423 (1969).  
<sup>30</sup> D.J. Scalapino, Phys. Rev. Lett. **24**, 1052 (1970).  
<sup>31</sup> H. Takayama, Prog. Theor. Phys. **46**, 1 (1971).  
<sup>32</sup> S.R. Shenoy and P.A. Lee, Phys. Rev. B **10**, 2744 (1974).  
<sup>33</sup> M. Cini, Solid State Commun. **20**, 605 (1976).  
<sup>34</sup> G.A. Sawatzky, Phys. Rev. Lett. **39**, 504 (1977).  
<sup>35</sup> M. Cini and C. Verdozzi, Solid State Commun. **57**, 657 (1986).  
<sup>36</sup> For a review, see C. Verdozzi, M. Cini, and A. Marini, J. Electron Spectrosc. Rel. Phenom. **117**, 41 (2001).  
<sup>37</sup> K. Winkler, G. Thalhammer, F. Lang, R. Grimm, J. Hecker Denschlag, A.J. Daley, A. Kantian, H.P. Büchler, and P. Zoller, Nature **441**, 853 (2006).  
<sup>38</sup> G. Seibold, F. Becca, and J. Lorenzana, Phys. Rev. Lett. **100**, 016405 (2008).  
<sup>39</sup> V. M. Galitskii, Zh. Eksp. Teor. Fiz. **34**, 14 (1958); [Sov. Phys. JETP **7**, **104** (1958)].  
<sup>40</sup> J. Kanamori, Prog. Theor. Phys. **30**, 275 (1963).  
<sup>41</sup> R. Frésard and P. Wölfle, Int. J. Mod. Phys. B **6**, 237 (1992).  
<sup>42</sup> B.R. Bulka, Phys. Stat. Sol. B **180**, 401 (1993).  
<sup>43</sup> B.R. Bulka and S. Robaszkiewicz, Phys. Rev. B **54**, 13138 (1996).  
<sup>44</sup> M. Bak and R. Micnas, J. Phys.: Condens. Matter **10**, 9029 (1998).  
<sup>45</sup> J.O. Sofo and C.A. Balseiro, Phys. Rev. **45**, 377 (1992).  
<sup>46</sup> J. Bünemann, F. Gebhard, K. Radnóci, and P. Fazekas, J. Phys. Condens. Matter **17**, 3807 (2005).  
<sup>47</sup> P. Ring and P. Schuck, *The nuclear many-body problem* Springer-Verlag, New York, 1980.  
<sup>48</sup> J. Blaizot, G. Ripka *Quantum theory of finite systems*, MIT Press, 1986.  
<sup>49</sup> D.J. Thouless, Nucl. Phys. **22**, 78 (1961).  
<sup>50</sup> W.F. Brinkman and T.M. Rice, Phys. Rev. B **2**, 4302 (1970).



- <sup>51</sup> R. Micnas, J. Ranninger, and S. Robaszkiewicz, *Rev. Mod. Phys.* **62**, 113 (1990).
- <sup>52</sup> J. Lorenzana, G. Seibold, and R. Coldea, *Phys. Rev. B* **72**, 224511 (2005).
- <sup>53</sup> G.D. Mahan, *Many Particle Physics*, Plenum, New York, 1990.
- <sup>54</sup> A. L. Fetter and J. D. Walecka, *Quantum theory of Many Particle Systems*, McGraw-Hill, New York, 1971.
- <sup>55</sup> R. Jastrow, *Phys. Rev.* **98**, 1479 (1955).
- <sup>56</sup> Recently, the role of the long-range Jastrow factor for having an accurate variational wave function in the Hubbard model has been discussed by M. Capello, F. Becca, M. Fabrizio, S. Sorella, and E. Tosatti, *Phys. Rev. Lett.* **94**, 026406 (2005).
- <sup>57</sup> E. Dagotto, *Rev. Mod. Phys.* **66**, 763 (1994).
- <sup>58</sup> F. Günther and G. Seibold, *Physica C* **460-462**, 1041 (2007).
- <sup>59</sup> L. Fallani, J.E. Lye, V. Guarrera, C. Fort, and M. Inguscio, *Phys. Rev. Lett.* **98**, 130404 (2007).